

# LOW LOSS WIRE DESIGN FOR THE DISCORAP DIPOLE\*

G. Volpini<sup>#</sup>, F. Alessandria, G. Bellomo, M. Sorbi, INFN Milano, LASA Laboratory, Italy  
 P. Fabbriatore, S. Farinon, R. Musenich, INFN Genova, Italy  
 U. Gambardella, INFN LNF, Italy  
 J. Kaugerts, G. Moritz, M. N. Wilson, GSI, Darmstadt, Germany

## Abstract

The SIS-300 synchrotron of the new FAIR facility at GSI (Germany) will use fast-cycled superconducting magnets. Its dipoles will be pulsed at 1 T/s; for comparison, LHC is ramped at 0.007 T/s and RHIC at 0.042 T/s. Within the frame of a collaboration between INFN and GSI, INFN has funded the project DISCORAP (*DIpoli SuperCONDuttori RAPidamente Pulsati*, or Fast Pulsed Superconducting Dipoles) whose goal is to design, construct and test a half-length (4 m), curved, model of one lattice dipole. This paper focuses on the low loss superconducting wire design, and in particular to the transverse resistivity calculations and the dynamic stability verification.

## WIRE CHARACTERISTICS

INFN has awarded a contract for the manufacture of five unit lengths of superconducting Rutherford cable for the DISCORAP dipole model magnet [1]; two units will have a larger filament diameter, and three a smaller one (see Table 1); these will be referred to as 1<sup>st</sup> and 2<sup>nd</sup> generation, respectively. Only two units are strictly required for the magnet manufacture and this redundancy should allow the comparison of different wire design solutions and to face manufacture problems.

The main characteristics of the superconducting wire are described in Table 1.

A cross section of the wire is shown in Fig. 1. The coloured zones represent the inter-bundle barriers, the hexagons represent the filamentary zones, with NbTi filaments embedded in a CuMn matrix both in the 1<sup>st</sup> and in the 2<sup>nd</sup> generation. The rest of the wire is in high-purity copper.

Besides having filaments with different diameters, the two generations have different bundle barrier material: the 1<sup>st</sup> generation in Cu and the 2<sup>nd</sup> generation in CuMn.

Table 1: Wire Main Characteristics

Diameter after coating	0.825 ± 0.003	mm
Filament twist pitch	5 +0.5 -0	mm
Effective Filament Diameter	1 <sup>st</sup> generation	3.5 μm
	2 <sup>nd</sup> generation	2.5 μm
Interfilament matrix material	Cu-0.5 wt% Mn	
I <sub>c</sub> @ 5 T, 4.22 K	> 541	A
ρ <sub>t</sub> at 4.22 K	0.4 + 0.09 B [T]	nΩ·m
Cu+CuMn:NbTi ratio (α)	>1.5 ± 0.1	

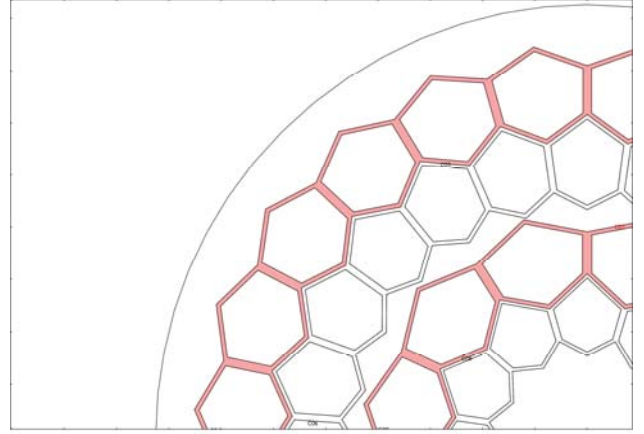


Figure 1: A detail of the wire cross section.

## LOSSES EDDY & TRANSVERSE CURRENTS

### Problem Statement

The largest loss contribution comes from the hysteretic losses within superconducting filaments. These losses are proportional to the filament diameter, and this motivates the quest for smaller filaments.

A second contribution is represented by the losses generated by Joule dissipation in the resistive matrix due to the currents induced by a changing external magnetic field, normal to the wire axis. These currents flow:

i) In loops composed by different superconducting filaments and closed through the matrix, in a plane normal to the wire axis. These are the interfilamentary currents;

ii) In circuits lying in planes parallel to the wire axis, entirely in the resistive matrix. These are the eddy-currents.

The contribution from i) + ii) to the power loss per unit volume is given by (in W/m<sup>3</sup>):

$$q = j^2 / \sigma = \sigma [\dot{B}^2 x^2 + (\partial_x \phi)^2 + (\partial_y \phi)^2] \quad (1)$$

( $\dot{B}$  is the external magnetic field ramp rate,  $\sigma$  is the resistive matrix conductivity and  $x$  the direction normal to the magnetic field and to the wire axis), where the first term between square parentheses accounts for the eddy currents, and the gradient terms describe the interfilamentary currents.

The potential can be computed from the Laplace's equation,

$$\nabla^2 \phi(x, y) = 0 \quad (2)$$

\*Work supported by INFN and partly by GSI

<sup>#</sup> Email: [giovanni.volpini@mi.infn.it](mailto:giovanni.volpini@mi.infn.it)

with proper boundary conditions:

$$\partial_n \varphi(R_0, \mathcal{G}) = 0$$

which describe the confinement of the currents inside the wire ( $R_0$  is its radius), and

$$\varphi_{BC}(R, \mathcal{G}) = \frac{\dot{B} L R}{2 \pi} \cos(\mathcal{G})$$

( $L$  is the filament twist pitch) valid on the filamentary zone boundaries, which takes into account the current entering/exiting into/from the filaments.

Once the total power dissipation  $Q$  found integrating Eq. 1 over the wire cross section has been computed, we express it in terms of transverse resistivity by means of

$$\rho_t = \frac{\dot{B}^2}{Q} \left( \frac{L}{2\pi} \right)^2$$

We therefore emphasize that we use the term “transverse resistivity” in a broader meaning, to describe both the sources i) and ii) of dissipation described above.

### Solving the Problem: Analytical Approach

Duchateau *et al.* [2] have developed a model, based on a simplified geometry, with cylindrical symmetry. In this model, equations (1) and (2) may be solved analytically.

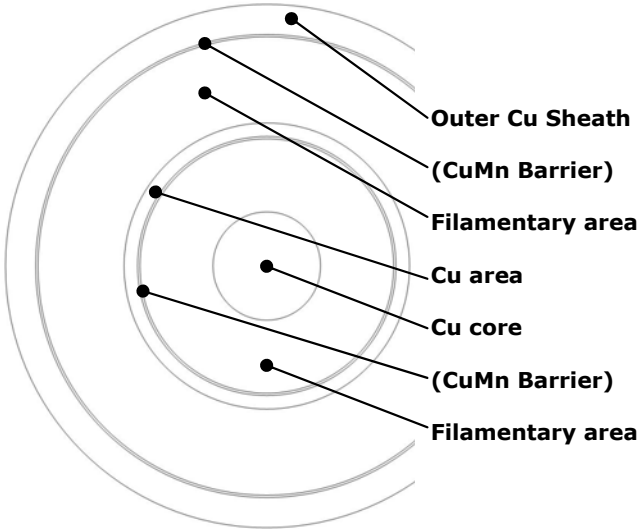


Figure 2: Annular region geometry model for the wire.

We have improved their approach, to better suit our geometry, increasing the number of annular regions from 4 to 7 (see Fig. 2). The Laplace equation has then been solved, and the power term integrated explicitly.

### Solving the Problem: FEM Solution

Equations (1) and (2) were solved also by means of a FEM simulation, performed with COMSOL 3.4. This allows a more realistic description of the wire geometry. In Fig. 3 we show the potential  $\varphi$  (colour map), and the current density due to the interfilament coupling, for a second generation wire, where both the barriers (shown in Fig. 1) are in CuMn. The total power dissipation  $Q$  is

found by numerical integration of (1). From  $Q$  we compute the effective transverse resistivity.

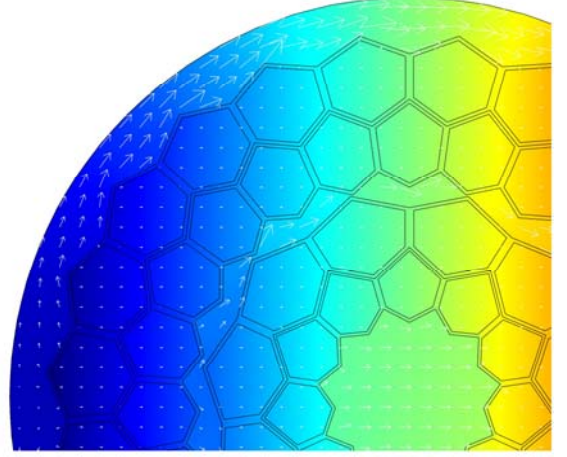


Figure 3: Coupling currents (white arrows) and coupling potential colour map for a 2<sup>nd</sup> generation wire.

### Comparison of the Analytical and FEM Results

Fig. 4 shows a comparison of the transverse resistivity values obtained with the analytical and FEM methods: we notice that have a good agreement, 15% or better, between the two approaches, the FEM results being always lower than those obtained from the analytical methods. This is a very good results, since the geometry approximation done in the analytical model is rather crude, as it can be appreciated comparing Fig. 1 and Fig. 2.

The computations have been done under two extreme hypotheses regarding the contact resistance between the NbTi filaments and the CuMn, referred to as “good coupling” and “poor coupling” in Fig. 4; in the former this resistance is zero and therefore the NbTi acts as a “shortcut” for the transverse current, while in the latter the contact resistance is very high, and the NbTi does not contribute at all to the transverse current flow. The uncertainty on the precise value of filament/matrix contact resistance introduces a discrepancy from 8% to 28% on the transverse resistivity.

From Fig. 4 we see that the 2<sup>nd</sup> generation is expected to have a transverse resistivity about 50% higher than the first one, at all fields.

In all the cases the results comply with the specification value reported in Table 1, represented here by the black line.

The contribution from eddy-currents to the total losses for  $\dot{B} = 1$  T/s, ranges from 10% to 15%, depending on the hypotheses.

We have also considered a further possibility, with only the outer barrier in CuMn and the inner one in Cu. The computed values of transverse resistivity are also shown in Fig. 4, for  $B = 5$  T, marked with a dot. We will not pursue this solution, since its performances appear too close to the 1<sup>st</sup> generation.

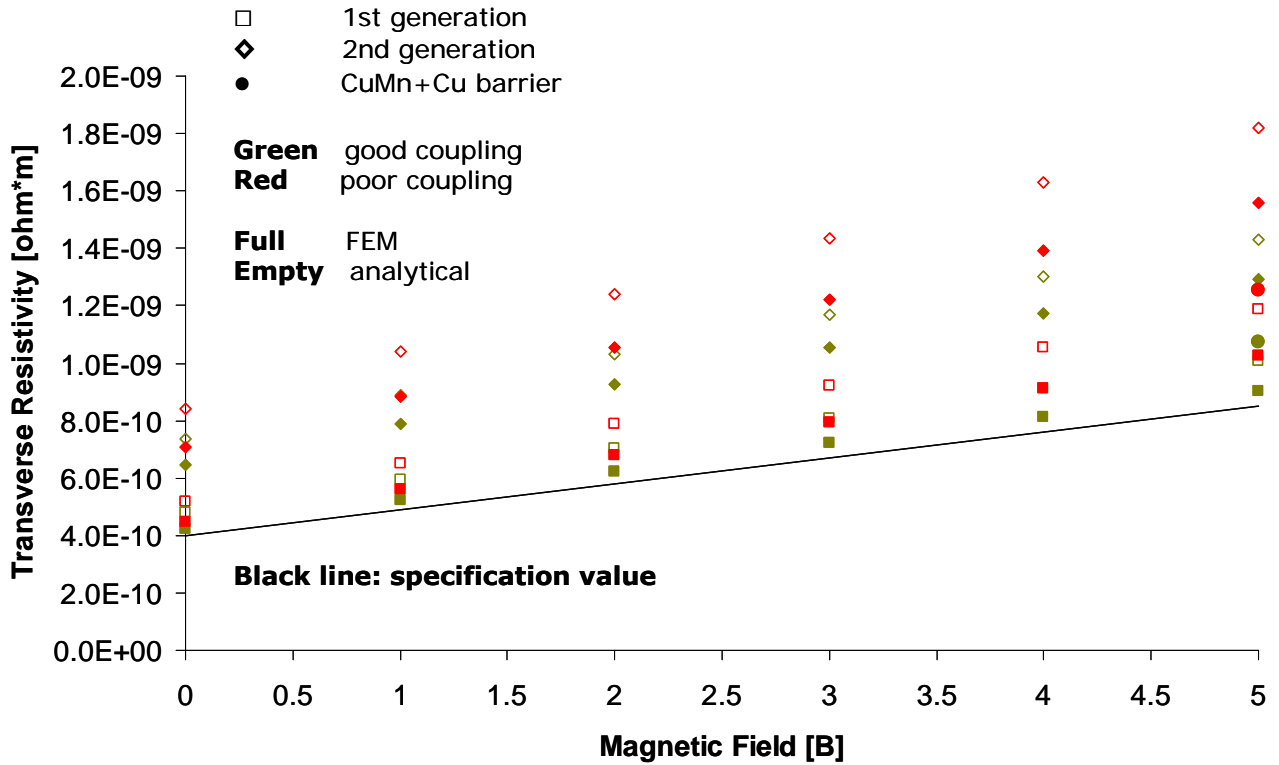


Figure 4: Comparison of transverse resistivity from analytical and FEM methods.

## WIRE DYNAMIC STABILITY

We investigate the thermal stability following the approach described in [3], [4]. In this context the critical element is represented by a single filamentary bundle, whose width must satisfy:

$$D_{bundle} < D_{max} = 4\sqrt{2} \sqrt{\frac{k_{th} \Delta\theta (1-\lambda)}{\lambda J_c^2 \rho_{el}}}$$

where:  $k_{th}$  is the filamentary bundle thermal conductivity, estimated assuming a weighed average between NbTi and CuMn yielding 1.9 W/mK;  $\Delta\theta$  is the temperature margin;  $\lambda$  is the NbTi fill factor in the filamentary bundle, 0.588;  $J_c$  is the critical current @ 4.2 K, 5 T, 2700 A/mm<sup>2</sup>;  $\rho_{el}$  is the matrix copper resistivity @ 4.2 K, 5 T,  $3.5 \cdot 10^{-10} \Omega \cdot m$ .

With these numbers  $D_{max} = 137 \mu m$ ; the bundle area width is 60–70  $\mu m$ , which is reasonably smaller than  $D_{max}$ ; the margin for stability seems comparable to that of the layouts envisaged by [3].

## CONCLUSIONS

Low-loss, fine filaments NbTi Rutherford cable is now manufactured by Luvata Fornaci di Barga (Italy) for the pulsed dipole long model, under contract from INFN.

Two generations of wire are foreseen, the first with 3.5  $\mu m$  filaments and the second with 2.5  $\mu m$  filaments. Transverse resistivity has been computed by means of

two different methods, one analytical and a FEM, and their results are in good agreement.

Larger uncertainties arise from unknown features, like the precise value of the contact resistance between the CuMn matrix and the NbTi filaments.

All the results comply with the transverse resistivity specified by DISCORAP.

## REFERENCES

- [1] G. Volpini *et al.*, “Low-Loss NbTi Rutherford Cable for Application to the SIS-300 Dipole Magnet Prototype”; IEEE Trans. Appl. Supercond., 18, Issue 2, June 2008 pp 997-1000
- [2] J. L. Duchateau, B. Turck and D. Ciazynski, “Coupling current losses in composites and cables: analytical calculations”, Ch. B4.3 in “Handbook of Applied Superconductivity”, IoP 1998.
- [3] M. N. Wilson, GSI Fast-Pulsed Synchrotron Project Report no. 29-2, Apr. 26, 2007.
- [4] M. N. Wilson, Superconducting Magnets, p 156, Clarendon Press, Oxford 1983.